PROCEEDINGS OF SCIENCE

ONLINE ICRC 2021
THE ASTROPARTICLE PHYSICS CONFERENCE
Berlin | Germany
37th International Cosmic Ray Conference
12–23 July 2021

FOV direction and image size calibration of Fluorescence Detector using light source on UAV

Arata Nakazawa,[a,*] **Takayuki Tomida,**[a] **Kengo Sano,**[a] **Yuichiro Tameda,**[b] **Yuya Oku**[b] **and Daisuke Ikeda**[c] **on behalf of the Telescope Array Collaboration**
(a complete list of authors can be found at the end of the proceedings)

[a] *Academic Assembly School of Science and Technology Institute of Engineering, Shinshu University, Nagano, Nagano, Japan*

[b] *Department of Engineering Science, Faculty of Engineering, Osaka Electro-Communication University, Neyagawa-shi, Osaka, Japan*

[c] *Faculty of Engineering, Kanagawa University, Yokohama, Kanagawa, Japan*

E-mail: 20w2066a@shinshu-u.ac.jp

In the Telescope Array (TA) experiment, we have been observing cosmic rays using a Fluorescence Detector (FD). More than 10 years have passed since we started this observation, and the accuracy of the observation has become more important than ever. We have developed the "Opt-copter" as a calibration device for the FDs. The Opt-copter is an unmanned aerial vehicle (UAV) equipped with a light source and can fly freely within the FD's field of view (FOV). In addition, the Opt-copter is equipped with a high-precision RTK-GPS, which enables it to accurately determine the position of the light source in flight. With this device, we can obtain detailed information on the optical properties of the FDs. So far, we have reported on the configuration of the device and the analysis of the FOV direction. In this presentation, we will report on the new FOV analysis and image size analysis.

37th International Cosmic Ray Conference (ICRC 2021)
July 12th – 23rd, 2021
Online – Berlin, Germany

*Presenter

PoS(ICRC2021)196

1. Introduction

The Telescope Array (TA) experiment, located in Utah, USA, aims to observe ultra-high energy cosmic rays at energies above $10^{18}eV$. The TA uses two types of detectors: the Fluorescence Detector (FD) that measures photons emitted from air molecules along a cosmic ray, and the Surface Detector (SD) that measures shower particles on the ground. The TA detector has been in operation for than 10 years [1][2]. Therefore, it is necessary to make observations with higher precision than before.

This report deals with the calibration systems for the TA FDs. The accuracy of the optical properties and PMT gain is important in determining cosmic ray parameters such as arrival direction, energy and X_{max}. We have developed "Opt-copter" as a FD calibration device using high intensity UV-LEDs mounted on the Unmanned Aerial Vehicle (UAV) [3]. Its position stability and portability allow to adjust the FD's optical system with excellent pointing accuracy with a single standard light source for all the FDs in 3 locations each $35km$ apart. A conceptual diagram of this device (Opt-copter) is shown in the Fig. 1.

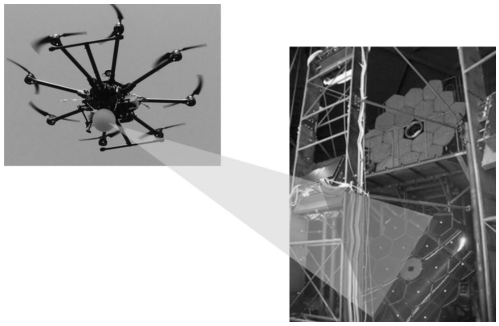

Figure 1: The conceptual diagram of measurement by Opt-copter.

Figure 2: The appearance of the Opt-copter that has eight arms, all of which are able to be folded. A GPS antenna is mounted on the top of this device.

2. The Opt-copter

The purpose of the Opt-copter is to grasp the optical properties of the FDs. The Opt-copter consists of a UAV, a light source, and a high-precision RTK-GPS module (Fig. 2). This device is flown $300m$ away from the FD during the measurement. The light source is a UV-LED with a wavelength of $375nm$, which emits light at $10Hz$ ~$30Hz$. The positional accuracy of RTK-GPS is typically $10cm$, which corresponds to a directional accuracy of $0.02°$.

2.1 Unmanned Aerial Vehicle (UAV)

We're mounting the light source on a high-stability 8-rotor helicopter (DJI S1000+). The size of the UAV is $400 \times 400 \times 500mm^3 (W \times D \times H)$ when the arms are collapsed, and its portability

with automatic leg and centrifugal propeller folding mechanism helps works in wilderness at night. This UAV allows both manual control and programmed flight path control. And it is equipped with a high-power and high- efficiency heat radiation motor and the all-carbon body frame of the vehicle. This S1000+ is also designed to load a camera for aerial photography, and we use this room (~$30cm^3$) to mount the light source and electronic devices. The maximum load weight is $7kg$. The flight controller (DJI A3) consists of a GPS and an attitude sensor to measure acceleration and atmospheric pressure. The positioning accuracy of S1000+ with A3 is about $3m$.

2.2 RTK-GPS

Because calibration accuracy varies greatly depending on how accurately measuring the position of the light source, the Opt-copter is equipped with RTK-GPS module for high precision positioning. For a PMT pointing calibration with the accuracy of 0.1°, a positioning accuracy of $0.5m$ is needed, and the Real Time Kinetic GPS (RTK-GPS) system (Swift Navigation, Piksi) enables this (Fig. 3). RTK-GPS uses two GPS modules, and records the relative position of the GPS antennas using the phase difference of the signals emitted from the GPS satellites. The position accuracy of RTK-GPS is typically $10cm$ after GPS calibration more than 1.5 hours. We evaluated the positioning accuracy on the ground. The RTK-GPS is tested the movement distance where was measured to $2m$ from the original point, and this measurement test that is 10 times trial. The RTK-GPS was tested for horizontally (East - West, North - South) and vertically, and the test of the above procedure for all of directions tests was performed 10 times. The distribution of the measured relative distances between the two modules is shown in Fig. 4, which exhibits that the horizontal and vertical accuracy of RTK-GPS is better than $10cm$. By loading one GPS module of RTK-GPS on the UAV and placing the other at a reference point on the ground where the position is previously measured in good accuracy, it is possible to know actual positions (the accuracy is better than 0.05°) of the UAV and the direction seen from the FDs.

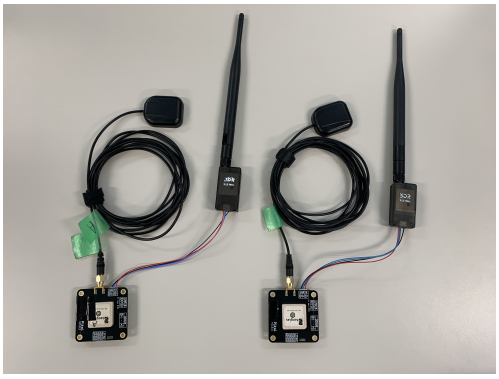

Figure 3: The Piksi is composed of two modules and records the relative position of them.

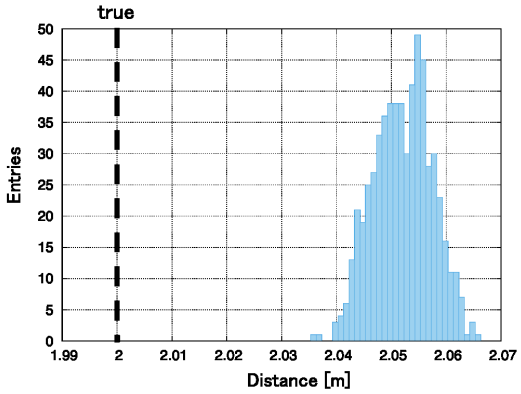

Figure 4: Ranging accuracy of RTK-GPS on the ground.

2.3 The triggering system

The TA FD consists of a composite light collecting mirror of $3.3m$ diameter and a 16×16 of PMTs (the camera) as shown in Fig. 1. The FD is designed to trigger the data acquisition system

when photons are detected with more than 5 adjoining PMTs within $25.6\mu s$ to detect cosmic ray showers, or by an external signal to the FD. Since the size of the Opt-copter light source image on the FD camera is as small as the size of a PMT, the self-triggering of FD does not work for Opt-copter signals. Therefore, we need a trigger generator for this to send trigger pulses both to FD and the light source in order that a measurement of the light source position, a UV-LED flash, and the FD data acquisition are made at the same time. The Opt-copter on flight position measures by the RTK-GPS as at the frequency of $10Hz$, and we use two GPS-based pulse generators of $10\tilde{}30Hz$: one on the Opt-copter for LED flashes, and the other is to trigger the FD data acquisition. This frequency is the maximum trigger rate of the FD in order to get as much data as possible. All the three GPS modules are presumably synchronized by the GPS-PPS signal every second. We compared the signal timing differences using an external high precision pulse generator that is also synchronized with GPS-PPS, and the GPS pulse for the Opt-copter as shown in Fig. 5. The distribution of the time differences between the two GPS-based pulse generators for the Opt-copter and for the FD trigger is presented in Fig. 6. This shows that the synchronization of the GPS-based pulse generator is as good as $0.1\mu s$, which is much smaller than the width of the UV-LED flash that is $10\mu s$.

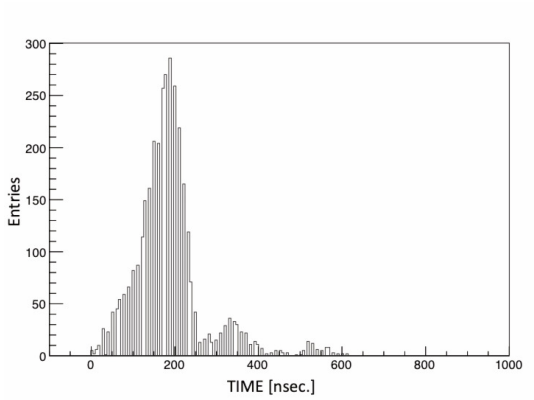

Figure 5: Time difference between pulse generator for light source and RTK-GPS measurement for ranging.

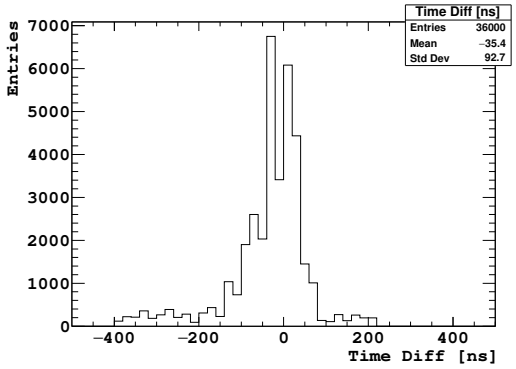

Figure 6: Time difference between the GPS-based pulse generators for FD trigger and the GPS-based pulse generator for the light source.

2.4 UV-LED light source

The optical system of the TA FD is optimized for photons of wavelengths between 300 and $400nm$, for fluorescence light from nitrogen and oxygen molecules. We use 12 UV-LEDs (Roithner Lasertechnik, H2A1-H375-E) at wavelength of $375nm$ for light source. The emission pattern of each LED is highly anisotropic, so we use a spherical light diffuser. Those LEDs are attached to each side of a dodecahedron created by a 3D printer and covered with a diffuser (Fig. 7).

3. Operation and Data

The position of the launching point of the Opt-copter ahead of each FD station is measured with good accuracy in advance. The light source is designed to be seen from the FD at the distance

Figure 7: The light source mounted on the Opt-copter is consisted of 12 UV-LEDs attached on dodecahedron and a spherical diffuser.

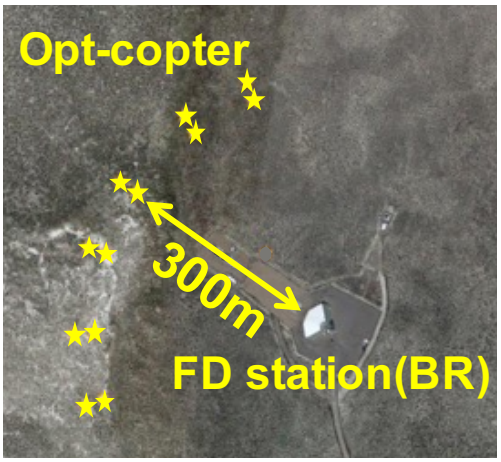

Figure 8: A bird's-eye view of the FD site taken by the flight.

of 300m, and the vehicle flies around in the field of view of the camera with a positioning accuracy of 10cm, which corresponds to a directional accuracy of 0.02°. Fig. 8 shows a bird's eye view of the FD site by an Opt-copter flight.

The measurement by the Opt-copter is measured from the FD and the RTK-GPS. The center of gravity (COG) is calculated from the amount of light received by each PMT and its center position. The COG is used as the light-receiving position of the FD. The RTK-GPS measures the relative position of the GPS antenna on the Opt-copter and the GPS antenna on the ground reference station. The ground reference station is a monument that has already been positioned by the measurement by another GPS module with high accuracy. To compare the two, we project the information by the RTK-GPS on the FD view (See Fig. 9). For the measurements made in 2019, we operated a uniform flight in the center of the FD's FOV for FOV direction analysis and real image size analysis. The trajectories of the detected the COG by the FD appear to be biased to the center of each PMT, which is different from the position of the projected image by the RTK-GPS measurement. If the image of the light source is sufficiently smaller than the size of one pixel of the FDs (PMT), the COG is biased towards the center of the PMT, which contains the main part of the image of the light source.

4. Analysis

4.1 FOV Direction analysis

Since the image size on the surface of the PMT array is small compared to a window size of the PMT, the COG is biased towards the center of the PMT which contains the main part of the image. Fig. 9 is the RTK-GPS positions projected on the focal plane and the COG positions. Fig. 10 is the difference between the RTK-GPS position and COG position in Fig. 9. And in Fig. 10, the red point is the mean of the green points. By statistically comparing the RTK-GPS position and the COG position as shown in Fig. 10, we can estimate the difference of the actual FOV direction to the assumed FOV direction of the FD. We performed this analysis for all the FDs of the BR station.

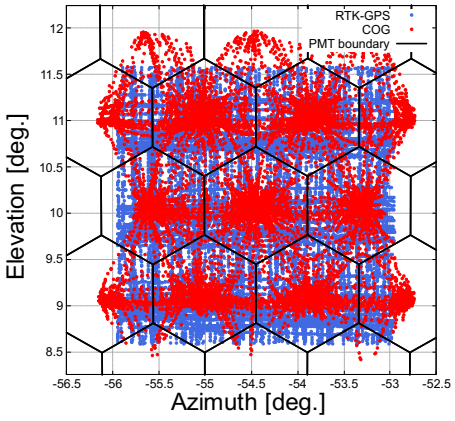

Figure 9: Measurement by RTK-GPS on FD viewing field and center of gravity of detected light by FD.

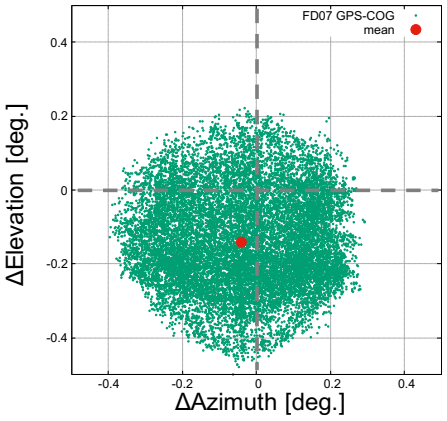

Figure 10: The difference between RTK-GPS position and the center of gravity position.

Table 1: The results of FOV direction analysis of the BR station (2018).

	FD00	FD01	FD02	FD03	FD04	FD05	FD06	FD07	FD08	FD09	FD10	FD11
ΔAzimuth [deg.]	0.05	0.00	0.04	0.04	0.04	0.02	0.01	-0.04	0.01	-0.05	-0.02	0.01
ΔElevation [deg.]	0.11	-0.04	0.02	-0.03	-0.04	-0.12	-0.05	-0.14	-0.12	-0.19	-0.14	-0.15

The results are shown in Table 1. It was found that most of the FDs were pointing downward more than expected. We also performed this analysis for each of the FD04 ~FD07 measurement data in 2018 and 2019 to check for reproducibility. The systematic error in this analysis is 0.03°, based on the systematic error in GPS position (0.02°) and FD (0.02°).

4.2 Image size analysis

We focused on the relationship between the RTK-GPS position and the light-receiving COG at the center of the FD's FOV as shown in Fig. 11. This relationship becomes stair-step with smaller image size on the surface of the PMT array. The axis in Fig. 11 and Fig. 12 shows the azimuthal opening between the RTK-GPS or COG position and the center of the PMT closest to the center of the FD's FOV. When the measurement by Opt-copter is simulated, the image size on the surface of the PMT array can be evaluated by comparing the simulation with the measurement data as shown in Fig. 11. Fig. 11 shows that the simulation roughly reproduces the measurement data and that we have a good understanding of the FD. A simple adjustment by eye level was also made to make the simulation further reproduce the measurement data, as shown in Fig. 12. The hit map of the photons in the simulation changed as shown in Fig. 13, and the image size on the surface of the PMT array was smaller than expected. In this way, the simulation can be made closer to the measurement data by using the Opt-copter. In the future, we will continue to analyze the effects of aberrations as well as the image size on the surface of the PMT array.

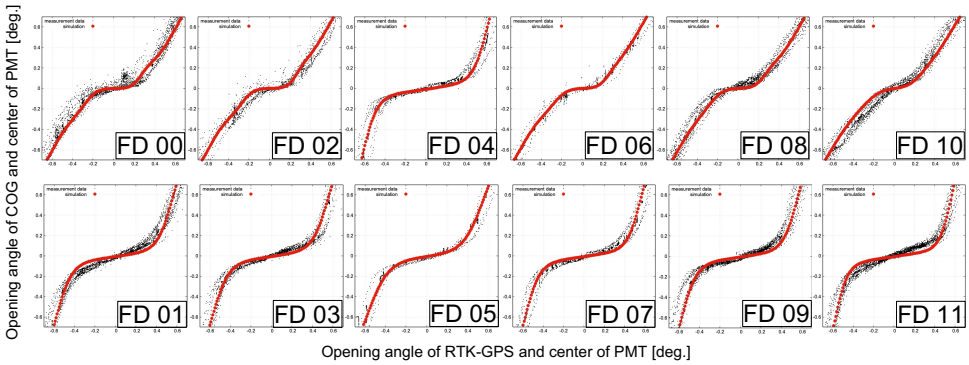

Figure 11: The relation ship between the RTK-GPS position and the COG position at the center of the FOV for the FD of the BR station (azimuthal).

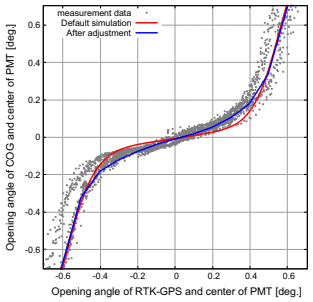

Figure 12: The changes in the relationship between the RTK-GPS position and the COG position before and after the simple adjustment (azimuthal).

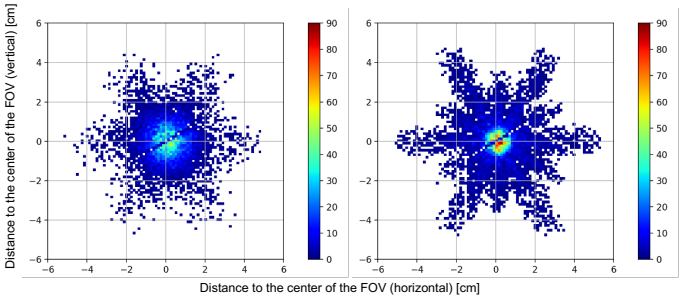

Figure 13: The hit map of photons at the center of the FD09's FOV. Left: Before adjustment. Right: After adjustment. Caution: These are affected by the PMT boundary.

5. Conclusion

The Opt-copter was developed as a calibration device for FDs. And by using the Opt-copter, we were able to estimate the assumed misalignment of the FOV direction of each FD with an accuracy of 0.03°. In addition, although we have a good understanding of the image size on the surface of the PMT array of each FD in the TA experiment, the Opt-copter allows us to understand it in even more detail. In the future, we need to estimate the impact of the results of the FOV direction analysis on the X_{max} analysis. And we will move from the image size analysis to aberration analysis.

6. Acknowledgements

The Telescope Array experiment is supported by the Japan Society for the Promotion of Science(JSPS) through Grants-in-Aid for Priority Area 431, for Specially Promoted Research JP21000002, for Scientific Research (S) JP19104006, for Specially Promoted Research JP15H05693, for Scientific Research (S) JP15H05741, for Science Research (A) JP18H03705, for Young Scientists (A) JPH26707011, and for Fostering Joint International Research (B) JP19KK0074, by the joint research program of the Institute for Cosmic Ray Research (ICRR), The University of

Tokyo; by the Pioneering Program of RIKEN for the Evolution of Matter in the Universe (r-EMU); by the U.S. National Science Foundation awards PHY-1404495, PHY-1404502, PHY-1607727, PHY-1712517, PHY-1806797 and PHY-2012934; by the National Research Foundation of Korea (2017K1A4A3015188, 2020R1A2C1008230, & 2020R1A2C2102800) ; by the Ministry of Science and Higher Education of the Russian Federation under the contract 075-15-2020-778, RFBR grant 20-02-00625a (INR), IISN project No. 4.4501.18, and Belgian Science Policy under IUAP VII/37 (ULB). This work was partially supported by the grants ofThe joint research program of the Institute for Space-Earth Environmental Research, Nagoya University and Inter-University Research Program of the Institute for Cosmic Ray Research of University of Tokyo. The foundations of Dr. Ezekiel R. and Edna Wattis Dumke, Willard L. Eccles, and George S. and Dolores Doré Eccles all helped with generous donations. The State of Utah supported the project through its Economic Development Board, and the University of Utah through the Office of the Vice President for Research. The experimental site became available through the cooperation of the Utah School and Institutional Trust Lands Administration (SITLA), U.S. Bureau of Land Management (BLM), and the U.S. Air Force. We appreciate the assistance of the State of Utah and Fillmore offices of the BLM in crafting the Plan of Development for the site. Patrick A. Shea assisted the collaboration with valuable advice and supported the collaboration's efforts. The people and the officials of Millard County, Utah have been a source of steadfast and warm support for our work which we greatly appreciate. We are indebted to the Millard County Road Department for their efforts to maintain and clear the roads which get us to our sites. We gratefully acknowledge the contribution from the technical staffs of our home institutions. An allocation of computer time from the Center for High Performance Computing at the University of Utah is gratefully acknowledged.

References

[1] H.Tokuno et al. ,NIM A, **676**, 54-65 (2012)

[2] T.Abu-Zayyad et al. ,NIM A, **689**, 87-97 (2012)

[3] T.Tomida et al. ,EPJ Web of Conferences **210**, 05015 (2019)

Full Authors List: Telescope Array Collaboration

R.U. Abbasi[1,2], T. Abu-Zayyad[1,2], M. Allen[2], Y. Arai[3], R. Arimura[3], E. Barcikowski[2], J.W. Belz[2], D.R. Bergman[2], S.A. Blake[2], I. Buckland[2], R. Cady[2], B.G. Cheon[4], J. Chiba[5], M. Chikawa[6], T. Fujii[7], K. Fujisue[6], K. Fujita[3], R. Fujiwara[3], M. Fukushima[6], R. Fukushima[3], G. Furlich[2], R. Gonzalez[2], W. Hanlon[2], M. Hayashi[8], N. Hayashida[9], K. Hibino[9], R. Higuchi[6], K. Honda[10], D. Ikeda[9], T. Inadomi[11], N. Inoue[12], T. Ishii[10], H. Ito[13], D. Ivanov[2], H. Iwakura[11], A. Iwasaki[3], H.M. Jeong[14], S. Jeong[14], C.C.H. Jui[2], K. Kadota[15], F. Kakimoto[9], O. Kalashev[16], K. Kasahara[17], S. Kasami[18], H. Kawai[19], S. Kawakami[3], S. Kawana[12], K. Kawata[6], I. Kharuk[16], E. Kido[13], H.B. Kim[4], J.H. Kim[2], J.H. Kim[2], M.H. Kim[14], S.W. Kim[14], Y. Kimura[3], S. Kishigami[3], Y. Kubota[11], S. Kurisu[11], V. Kuzmin[16], M. Kuznetsov[16,20], Y.J. Kwon[21], K.H. Lee[14], B. Lubsandorzhiev[16], J.P. Lundquist[2,22], K. Machida[10], H. Matsumiya[3], T. Matsuyama[3], J.N. Matthews[2], R. Mayta[3], M. Minamino[3], K. Mukai[10], I. Myers[2], S. Nagataki[13], K. Nakai[3], R. Nakamura[11], T. Nakamura[23], T. Nakamura[11], Y. Nakamura[11], A. Nakazawa[11], E. Nishio[18], T. Nonaka[6], H. Oda[3], S. Ogio[3,24], M. Ohnishi[6], H. Ohoka[6], Y. Oku[18], T. Okuda[25], Y. Omura[3], M. Ono[13], R. Onogi[3], A. Oshima[3], S. Ozawa[26], I.H. Park[14], M. Potts[2], M.S. Pshirkov[16,27], J. Remington[2], D.C. Rodriguez[2], G.I. Rubtsov[16], D. Ryu[28], H. Sagawa[6], R. Sahara[3], Y. Saito[11], N. Sakaki[6], T. Sako[6], N. Sakurai[3], K. Sano[11], K. Sato[3], T. Seki[11], K. Sekino[6], P.D. Shah[2], Y. Shibasaki[11], F. Shibata[10], N. Shibata[18], T. Shibata[6], H. Shimodaira[6], B.K. Shin[28], H.S. Shin[6], D. Shinto[18], J.D. Smith[2], P. Sokolsky[2], N. Sone[11], B.T. Stokes[2], T.A. Stroman[2], Y. Takagi[3], Y. Takahashi[3], M. Takamura[5], M. Takeda[6], R. Takeishi[6], A. Taketa[29], M. Takita[6], Y. Tameda[18], H. Tanaka[3], K. Tanaka[30], M. Tanaka[31], Y. Tanoue[3], S.B. Thomas[2], G.B. Thomson[2], P. Tinyakov[16,20], I. Tkachev[16], H. Tokuno[32], T. Tomida[11], S. Troitsky[16], R. Tsuda[3], Y. Tsunesada[3,24], Y. Uchihori[33], S. Udo[9], T. Uehama[11], F. Urban[34], T. Wong[2], K. Yada[6], M. Yamamoto[11], K. Yamazaki[9], J. Yang[35], K. Yashiro[5], F. Yoshida[18], Y. Yoshioka[11], Y. Zhezher[6,16], and Z. Zundel[2]

[1] Department of Physics, Loyola University Chicago, Chicago, Illinois, USA

[2] High Energy Astrophysics Institute and Department of Physics and Astronomy, University of Utah, Salt Lake City, Utah, USA

[3] Graduate School of Science, Osaka City University, Osaka, Osaka, Japan

[4] Department of Physics and The Research Institute of Natural Science, Hanyang University, Seongdong-gu, Seoul, Korea

[5] Department of Physics, Tokyo University of Science, Noda, Chiba, Japan

[6] Institute for Cosmic Ray Research, University of Tokyo, Kashiwa, Chiba, Japan

[7] The Hakubi Center for Advanced Research and Graduate School of Science, Kyoto University, Kitashirakawa-Oiwakecho, Sakyo-ku, Kyoto, Japan

[8] Information Engineering Graduate School of Science and Technology, Shinshu University, Nagano, Nagano, Japan

[9] Faculty of Engineering, Kanagawa University, Yokohama, Kanagawa, Japan

[10] Interdisciplinary Graduate School of Medicine and Engineering, University of Yamanashi, Kofu, Yamanashi, Japan

[11] Academic Assembly School of Science and Technology Institute of Engineering, Shinshu University, Nagano, Nagano, Japan

[12] The Graduate School of Science and Engineering, Saitama University, Saitama, Saitama, Japan

[13] Astrophysical Big Bang Laboratory, RIKEN, Wako, Saitama, Japan

[14] Department of Physics, SungKyunKwan University, Jang-an-gu, Suwon, Korea

[15] Department of Physics, Tokyo City University, Setagaya-ku, Tokyo, Japan

[16] Institute for Nuclear Research of the Russian Academy of Sciences, Moscow, Russia

[17] Faculty of Systems Engineering and Science, Shibaura Institute of Technology, Minato-ku, Tokyo, Japan

[18] Department of Engineering Science, Faculty of Engineering, Osaka Electro-Communication University, Neyagawa-shi, Osaka, Japan

[19] Department of Physics, Chiba University, Chiba, Chiba, Japan

[20] Service de Physique Th$acutee$orique, Universit$acutee$ Libre de Bruxelles, Brussels, Belgium

[21] Department of Physics, Yonsei University, Seodaemun-gu, Seoul, Korea

[22] Center for Astrophysics and Cosmology, University of Nova Gorica, Nova Gorica, Slovenia

[23] Faculty of Science, Kochi University, Kochi, Kochi, Japan

[24] Nambu Yoichiro Institute of Theoretical and Experimental Physics, Osaka City University, Osaka, Osaka, Japan

[25] Department of Physical Sciences, Ritsumeikan University, Kusatsu, Shiga, Japan

[26] Quantum ICT Advanced Development Center, National Institute for Information and Communications Technology, Koganei, Tokyo, Japan

[27] Sternberg Astronomical Institute, Moscow M.V. Lomonosov State University, Moscow, Russia

[28] Department of Physics, School of Natural Sciences, Ulsan National Institute of Science and Technology, UNIST-gil, Ulsan, Korea

[29] Earthquake Research Institute, University of Tokyo, Bunkyo-ku, Tokyo, Japan

[30] Graduate School of Information Sciences, Hiroshima City University, Hiroshima, Hiroshima, Japan

[31] Institute of Particle and Nuclear Studies, KEK, Tsukuba, Ibaraki, Japan

[32] Graduate School of Science and Engineering, Tokyo Institute of Technology, Meguro, Tokyo, Japan

[33] Department of Research Planning and Promotion, Quantum Medical Science Directorate, National Institutes for Quantum and Radiological Science and Technology, Chiba, Chiba, Japan

[34] CEICO, Institute of Physics, Czech Academy of Sciences, Prague, Czech Republic

[35] Department of Physics and Institute for the Early Universe, Ewha Womans University, Seodaaemun-gu, Seoul, Korea

PoS(ICRC2021)196